

ALTITUDE EFFECTS ON HIGH-TIME RESOLUTION MEASUREMENTS OF VEHICLE CHARGING DUE TO ELECTRON EMISSION AT LEO ALTITUDES

Neil B. Myers* and W. John Raitt
Center for Atmospheric and Space Sciences
Utah State University

*now at Rome Air Development Center
Hanscom AFB, MA

Spacecraft Charging Technology Conference
Naval Postgraduate School
October 31-November 3, 1989

Abstract. Transient vehicle potential was measured during the CHARGE-2 electron beam experiment using a tethered payload as an electrical reference. Measurements of transient vehicle potential were obtained at sample intervals as short as 100 ns. Above 220 km transient potentials increased monotonically. Below 220 km the transient potential reached a maximum 50 μ s after initiation of beam emission and then decreased. Beam-neutral and beam-plasma interactions are thought to be responsible for the decrease in vehicle potential below 220 km.

Introduction

Electron beam experiments have been performed in the ionosphere using sounding rockets since 1969 [Hess *et al.*, 1971]. The success of these experiments in emitting electron beams contradicted the predictions of some models that predicted severe restrictions on the amount of current that could be collected from the ionosphere [Parker and Murphy, 1961]. According to the models, a vehicle which emitted too large of a current (depending on the area of the vehicle) would not be able to collect a sufficient current to balance the emitted current and the potential of the vehicle would rise to that of the accelerating potential of the electron gun preventing further emission. The successful emission of currents larger than the theoretical limitations stimulated interest in understanding the processes that occur during electron beam emission that provide the return current to the vehicle. A large number of electron beam experiments were performed using sounding rockets [Winckler, 1980], but unambiguously measuring both the vehicle potential and the collected current proved difficult. The Cooperative High Altitude Rocket Gun Experiment

(CHARGE) series was designed to compare the current collection of a vehicle in the ionosphere at high potential both with and without electron beam emission. During the successful flight of the CHARGE-2 experiment it was found that without electron beam emission the collected current was magnetically limited as predicted by Parker and Murphy [Myers *et al.*, 1989]. However the electron emission process greatly enhanced the current collection at low altitude (below 240 km). Measurements of vehicle potential with high time resolution were performed to aid in understanding the processes that allow the electron beam to generate sufficient electron return current and will be the subject of this paper.

Experiment

The CHARGE-2 experiment was launched December 14, 1985 just after local midnight from White Sands Missile Range, New Mexico. The main payload carried the electron beam and most of the diagnostic instrumentation and was referred to as the mother. A portion of the vehicle was deployed up to 426 m from the mother, connected by a conducting insulated tether, and was referred to as the daughter. The 1-kV electron gun emitted beam currents from less than 1 mA to 48 mA. The electron beam was successfully emitted from altitudes of 115 to 262 km. The daughter payload served as a reference electrode for the mother potential during beam emission. A high time resolution data capture system was used to measure the beam current and vehicle potential with sample intervals as short as 100 ns. Many other instruments were flown as part of the experiment as can be seen in Figure 1. The scope of this paper is limited to the high time resolution measurements. Results from some of the other instrumentation have been reported by Myers *et al.*, (Vehicle charging effects during electron beam emission from the CHARGE-2 experiment, in press *J. Spacecraft and Rockets*, 1990) and Sasaki *et al.*, [1987].

During electron emission a sheath is formed around the beam-emitting vehicle. In addition, the region surrounding the vehicle is disturbed by the beam-emission process. This complicates the interpretation of vehicle potential by a probe inside of the sheath and the disturbed region. To avoid this complication the daughter was deployed outside of the sheath in a direction perpendicular to the geomagnetic field to remove it from the disturbed region. The mother potential was then measured referenced to the daughter potential during beam emission. The mother-to-daughter potential is equal to the mother potential with respect to the plasma if the daughter potential is small, as seen in Figure 2. This was the method used to make the high time resolution measurements of the mother vehicle potential during electron beam emission. The beam current was measured using a Rogowski coil with the same time resolution as the potential measurements. The tether current, which equals the current collected by the daughter, was measured at a sample

rate of 1250 s^{-1} . Thus the current collected by the mother was determined by subtracting the tether current from the beam current.

Results

Measurements using the high time resolution system were limited to capturing 1024 points, which filled the cache memory. Thus at a sample interval of 100 ns data were captured for a total window of 102 μs . The cache memory then took 0.82 seconds to dump to the telemetry system so further data could not be obtained for 0.82 seconds. The sample interval could be varied from 100 ns to 25.6 μs . Measurements of the electron beam current using the high time resolution system are shown in Figure 3. Beam current is shown versus time in microseconds after the triggering of the cache memory for a sample interval of 100 ns. The beam current rose to a fairly constant value after 400 ns. This demonstrates the fast rise time of the electron beam current.

Figure 4 shows beam current and mother potential versus time in microseconds using a sample interval of 100 ns, at an altitude of 260 km. The data in the panels on the left were obtained at the initiation of beam emission and show the beam current and potential for the first 100 μs of beam emission. The data in the panel on the right shows the second capture of data during the same beam emission obtained 0.82 s after initiation of beam emission and shows 100 μs of data after steady-state conditions prevailed. No beam current data can be obtained for steady state conditions since the Rogowski coil is an AC coupled current measuring device. The beam current rose quickly to a value of about 23 mA. The vehicle potential rose to 40 V within a few microseconds and then continued to increase to 60 V by the end of the 102 μs window for data capture. The potential must have continued to rise since the second panel of potential measurements indicates a value of 160 V for the potential difference between the mother and the daughter payloads. The potential measurements of the second panel do not represent the potential of the mother with respect to the plasma since the daughter has obtained a large potential with respect to the plasma within 0.82 s after the initiation of beam emission due to the low resistance between the mother and daughter (approximately 40 k Ω in this case). The first panel of potential measurements does represent the mother potential with respect to the plasma since the daughter cannot change potential quickly due to the capacitance of the tether (calculated to be 10^{-7} F). Thus the daughter could not obtain large potentials due to the mother's positive potential for times much less than 4 ms. The measurements of the second panel were obtained much more than 4 ms after the beam turn-on, so the daughter has had time to charge to a high positive potential. Measurements from the floating probe array 1 m from the mother skin indicate a steady-state mother potential of about 440 V with respect to the plasma at this time. This indicates that the

daughter obtained a potential of about 280 V with respect to the plasma during steady state.

Two separate beam emissions with a beam current of 3 mA are shown in Figure 5. Potential is shown versus time in microseconds after the beginning of beam emission. The data in the top panel were obtained with a sample interval of 1.6 μs while the data of the lower panel were obtained with a sample interval of 100 ns. The two beam operations occurred within one second of each other at 235 km. The potential was very small during the first 100 μs as seen in the lower panel but rose to about 40 V within 500 μs (upper panel). Low transient potentials were typical for the data above 200 km where the plasma density was relatively large (greater than 10^{10} m^{-3}). This is to be expected for low beam currents on the order of the thermal current to the vehicle.

A comparison of similar beam operations at different altitudes is shown in Figure 6. The mother-daughter potential is shown versus the time in microseconds after the start of the beam operation. The data obtained at 156 km were from a 2-mA beam emission, while the data obtained at 235 km were from a 3-mA beam operation. Both data sets were obtained with a 100-ns sample interval. The vehicle potential was larger for the low altitude data as would be expected due to the lower plasma density. The potential obtained at the lower altitude also showed a maximum value about 50 μs after the start of the beam operation, and then decreased for the remaining 50 μs of the data capture window.

A similar comparison of vehicle potential obtained at different altitudes is shown in Figure 7. In this case the data were obtained with a sample interval of 1.6 μs , allowing a data window of 1.6 ms. Both data sets were from a 1.5-mA beam operation. The high altitude data were obtained at 237 km and show a steadily increasing potential until 1 ms after the start of the beam emission. The low altitude data were obtained at 155 km and exhibits the same potential maximum about 50 μs after the start of the beam operation followed by a decreasing potential as seen the low altitude data from Figure 6.

High time resolution vehicle potential data were also obtained during pulsing beam operations, but only at low altitude. An example of this is shown in Figure 8 with beam current versus time in microseconds after the start of the beam pulsing operation in the top panel and potential versus time in the lower panel. The beam pulsed on for 4 μs and off for 4 μs . The sample interval was 200 ns and the data were obtained at 125 km. The 48-mA beam current was much larger than the previous examples using DC beam emissions. The vehicle potential shows the same maximum at 50 μs after the start of the pulsing operations followed by decreasing potentials for each successive beam pulse as seen in the previous examples of low altitude potential measurements. This same behavior was seen in other pulsing operations at low altitude regardless of the beam pulsing frequency.

Discussion

The measurements of the transient potential between the mother and daughter payloads due to electron beam emission were lower than the steady state measurements of the mother potential using the floating probes on a 1-m boom. Thus steady-state conditions were not reached for over 100 μs . This is much longer than it takes electrons to travel the meter-length sheath distance of the *Langmuir and Blodgett* [1924] type. This indicates that current collection in the ionosphere is more complicated than the simple space-charge-limited models. As shown by *Myers et al.*, [1989] current collection by a passive vehicle at high potential follows closely the magnetically limited model of *Parker and Murphy* [1961] which allows for the collection of electrons from large distances along the magnetic field lines. The large time until steady-state conditions were achieved supports this conclusion.

It was also shown by Myers that the process of electron beam emission can drastically affect the current collection of a high potential vehicle at altitudes below 240 km. The results of the transient measurements also support the conclusion that a different process becomes important at altitudes below 220 km. The small plasma density at these low altitudes prevents a large current from being collected in the vicinity of the vehicle, and initially the potential rises to large values until a subsequent decrease in potential 50 μs after the initiation of beam emission. Although the maximum potential occurs consistently at 50 μs for the low altitude data it is unlikely that this is due to charging of the daughter since this behavior is not seen for the high altitude data and the tether time constant should be on the order of milliseconds. The contribution due to ionization of neutrals by the sheath-accelerated electrons does not explain the decrease of potential because of the large amount of time involved. It is possible that $E \times B$ trapped electrons could continually increase to the point where they ionize a significant number of neutrals. However the pulsing beam operations would not be explained by this since the vehicle potential returned to plasma potential between pulses and would continually turn off the $E \times B$ process, preventing such a build up of density. Also a large number of trapped electrons would yield a different signature from the monotonic sheath which the sheath floating probes measured [*Myers et al.*, 1989]. The most likely explanations for this behavior at low altitude are the beam-plasma and beam-neutral interactions. Beam-plasma interactions should not be important initially since the decrease of potential at 50 μs occurs only at the low altitudes where plasma density is small. Neutral density is larger at the lower altitudes providing a greater probability that beam electrons will ionize the neutrals. The long time for the vehicle potential to decrease indicates that the neutrals are ionized at great distances from the rocket. The interaction of the electron beam with the neutral atmosphere at large distances is discussed by *Neubert et al.*, (The interaction of an artificial electron beam with the

Earth's upper atmosphere: Effects on spacecraft charging and the near-plasma environment, submitted to *J. Geophys. Res.*, 1990) and in a paper in this proceedings. It is possible that beam-plasma interactions play an increasing role in providing a return current once the beam electrons create a significant number of low energy electrons in the beam column.

Acknowledgements. The experimental work was sponsored with funds from NASA grant NAG5-607 and NAGW-1566 and funds from the Japanese government.

References

- Hess, W.N., M. G. Trichel, T. N. Davis, W. C. Beggs, G. E. Kraft, E. Stassinopoulos and E. J. R. Maier, Artificial auroral experiment: Experiment and principal results, *J. Geophys. Res.*, 76, 6067, 1971.
- Langmuir, I. and K. Blodgett, Current limited by space charge flow between concentric spheres, *Phys. Rev.*, 24, 49, 1924.
- Myers, N.B, W.J. Raitt, B.E. Gilchrist, P.M. Banks, T. Neubert, P.R. Williamson, S. Sasaki, A comparison of current-voltage relationships of collectors in the Earth's ionosphere with and without electron beam emission, *Geophys. Res. Lett.*, 16, 365, 1989.
- Parker, L. W. and B. L. Murphy, Potential buildup on an electron-emitting ionospheric satellite, *J. Geophys. Res.*, 72, 1631, 1967.
- Winckler, J. R., The application of artificial electron beams to magnetospheric research, *Reviews of Geophysics and Space Physics*, 18, 659, 1980.
- Sasaki, S., W. J. Raitt, K-I. Oyama, N. Kawashima, P. R. Williamson, W. F. Sharp, A. B. White, P. M. Banks, T. Yokota, Y. Watanabe, K. Hirao, and T. Obayashi, Results from a series of tethered rocket experiments, *AIAA Journal of Spacecraft and Rockets*, 24, 444, 1987.

Figure Captions

Figure 1. The CHARGE-2 payload configuration.

Figure 2. Potential distribution during electron beam emission.

Figure 3. High time resolution measurements of electron beam current.

Figure 4. High time resolution measurements of beam current and mother-daughter potential for two successive data captures during one DC beam operation at 260 km.

Figure 5. High time resolution measurements of vehicle potential for two separate 3-mA beam operations at 235 km. Sample interval is 1.6 μs (top panel) and 0.1 μs (lower panel).

Figure 6. High time resolution measurements of vehicle potential for a 2-mA beam operation at 156 km and a 3-mA operation at 235 km with a sample interval of 0.1 μs .

Figure 7. High time resolution measurements of vehicle potential for 1.5-mA beam operations at 155 km and 237 km with a sample interval of 1.6 μs .

Figure 8. High time resolution measurements of beam current (top panel) and vehicle potential (lower panel) for a pulsing beam operation at 125 km with a sample interval of 0.2 μs . The beam was on for 4 μs and off for 4 μs .

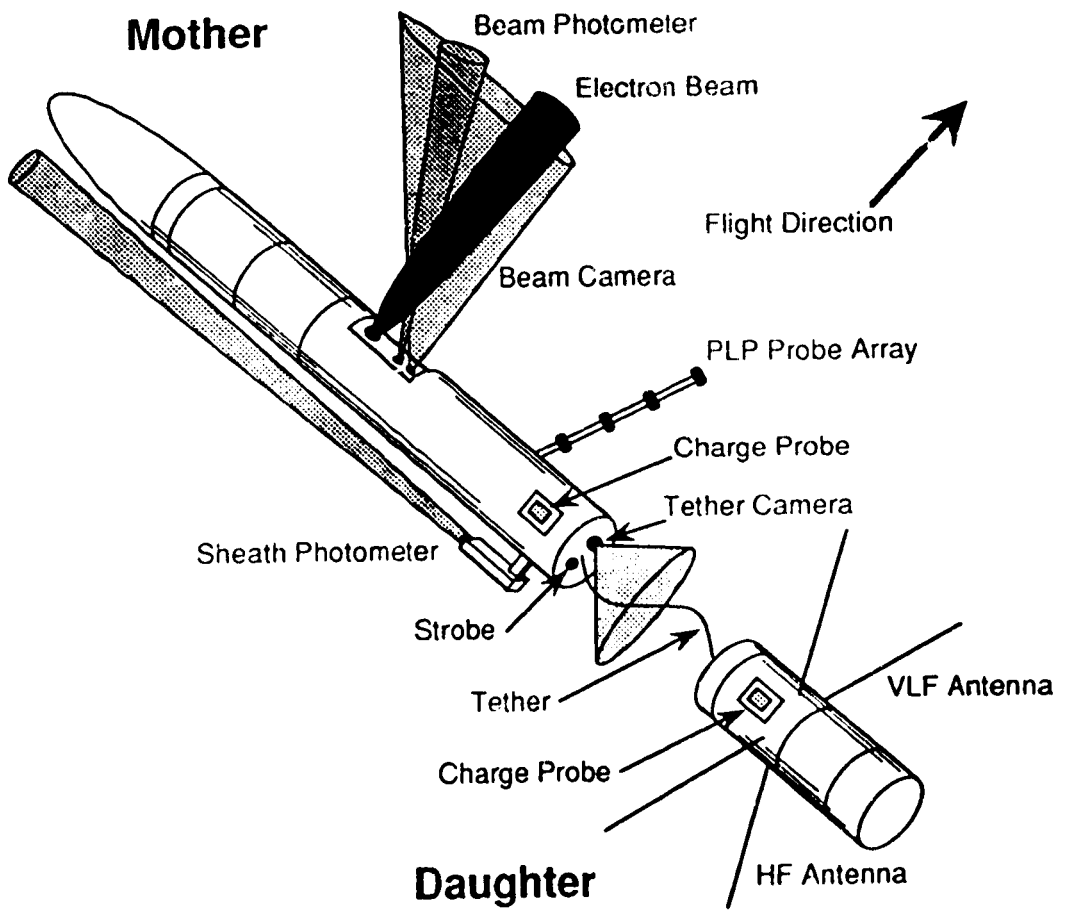


Figure 1

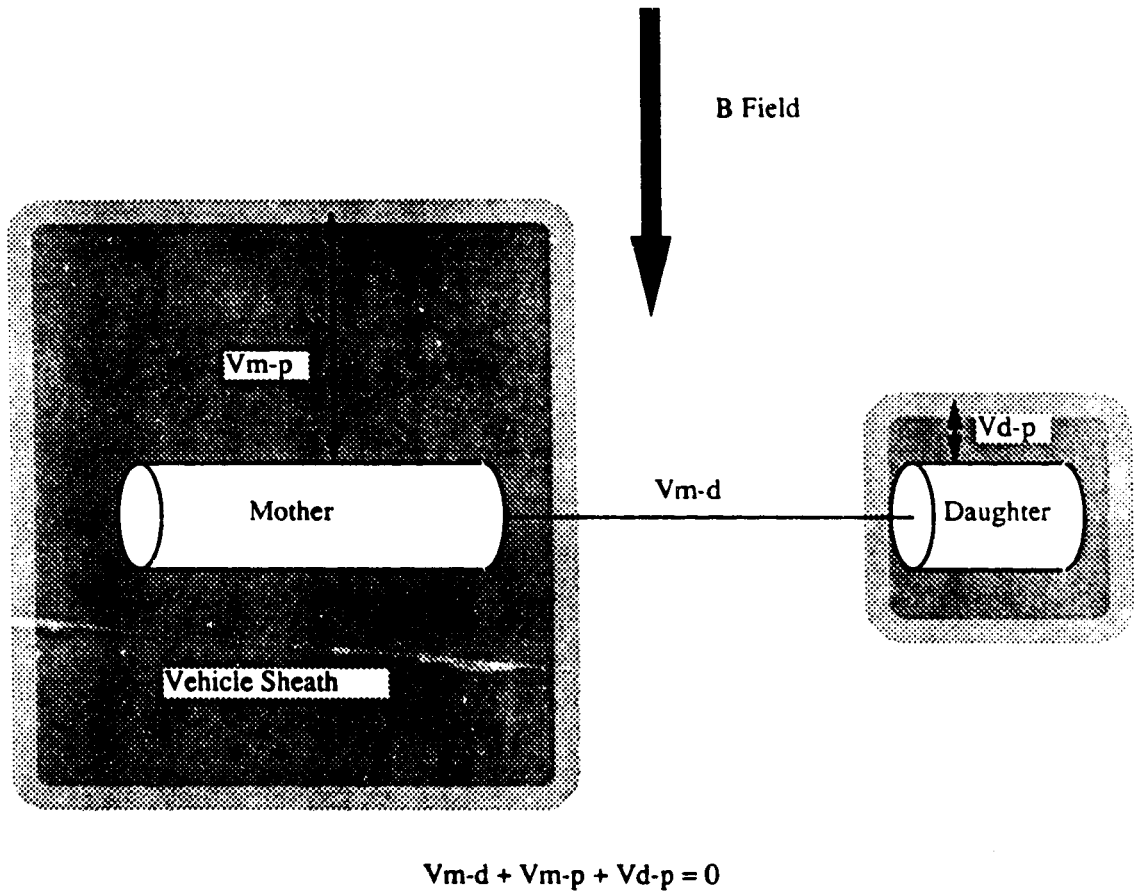


Figure 2

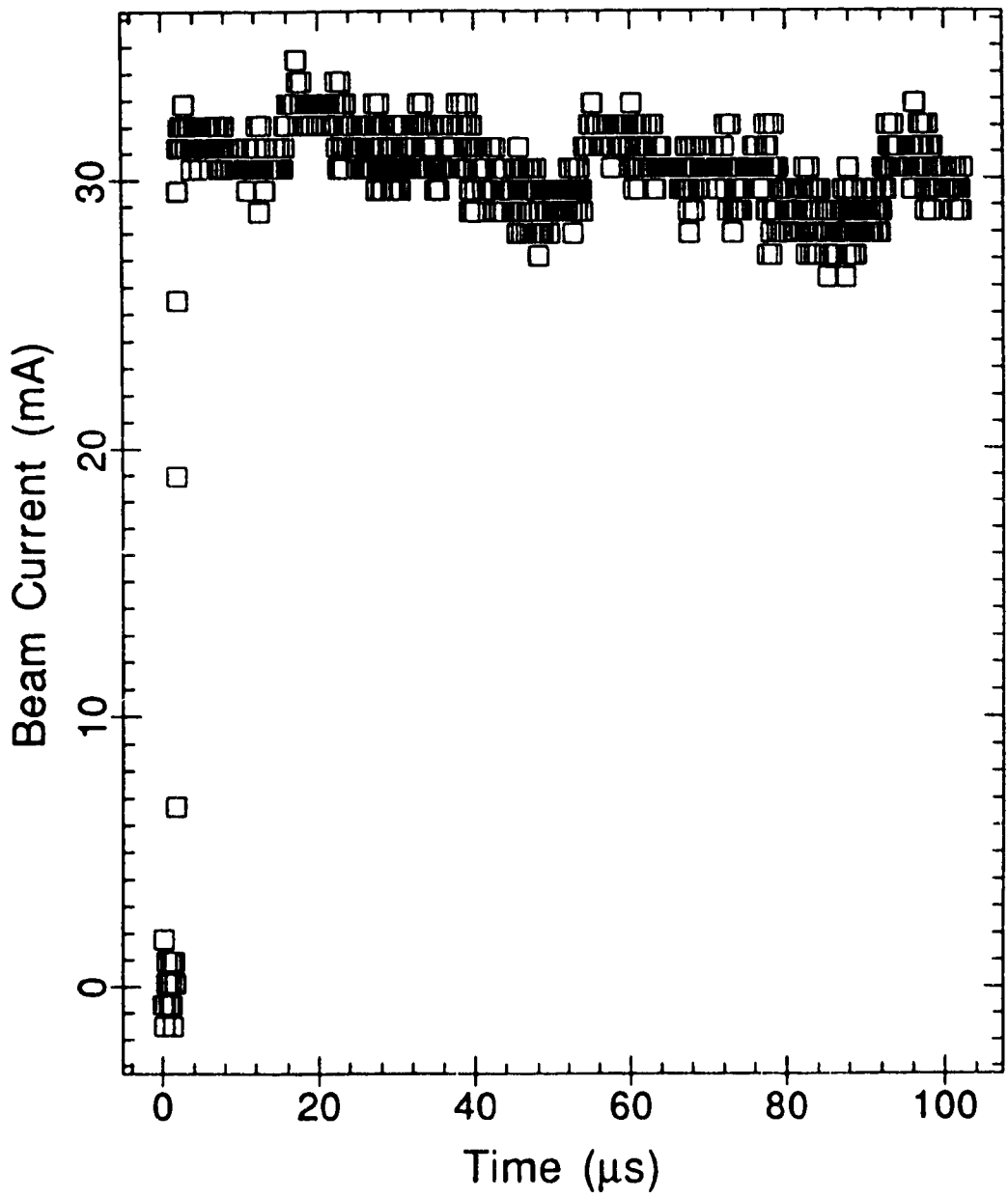
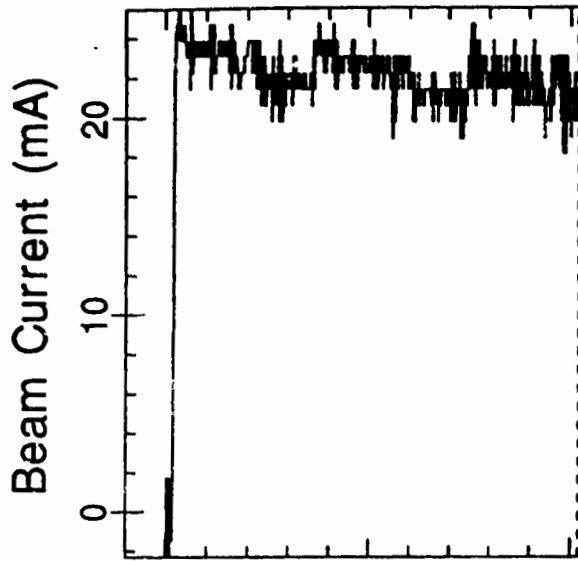


Figure 3



No Data

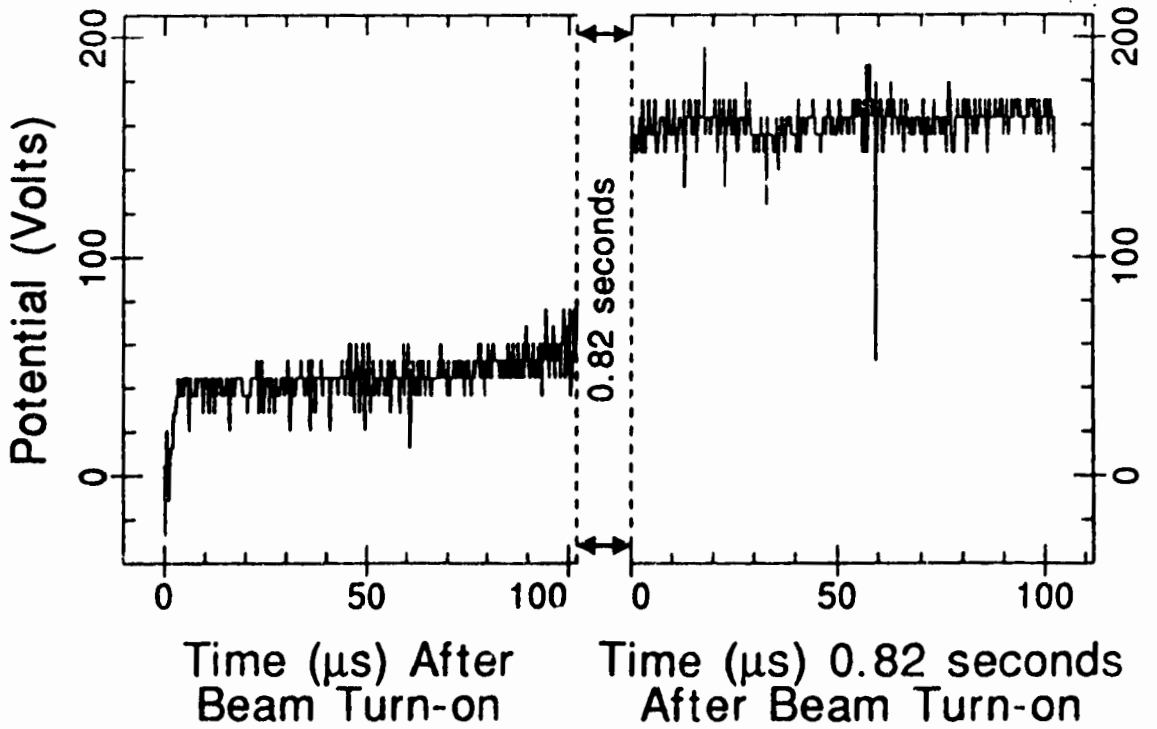


Figure 4

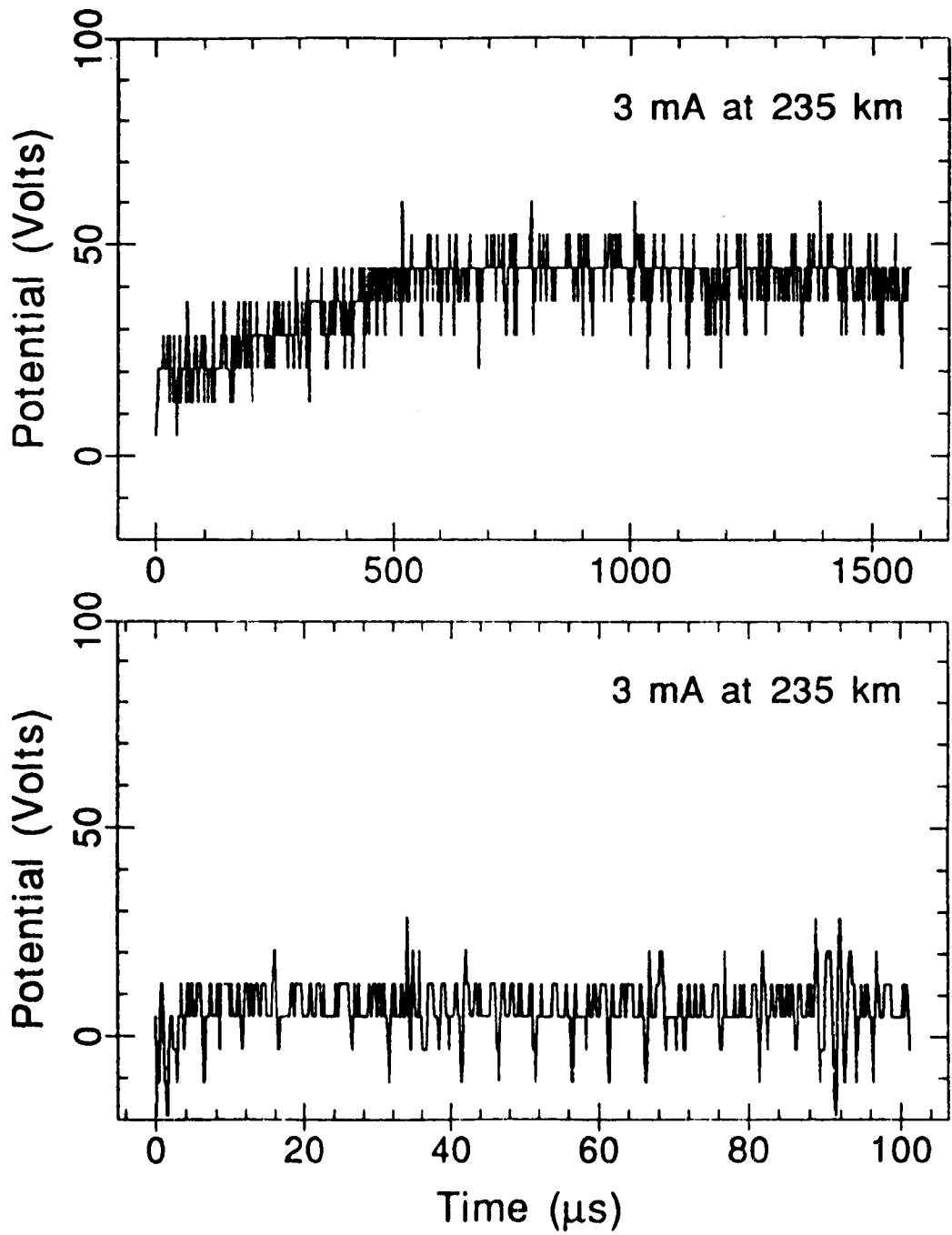


Figure 5

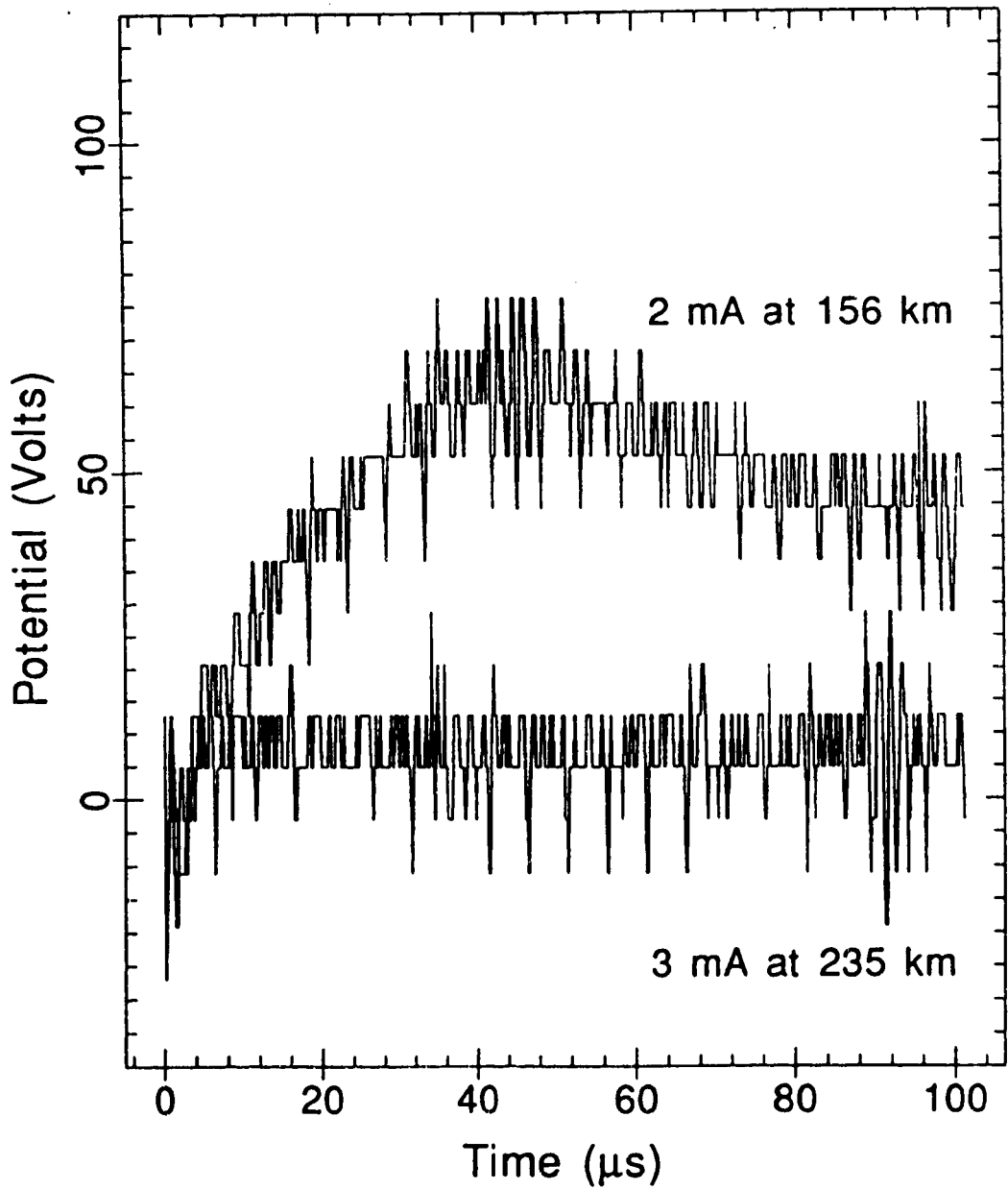


Figure 6

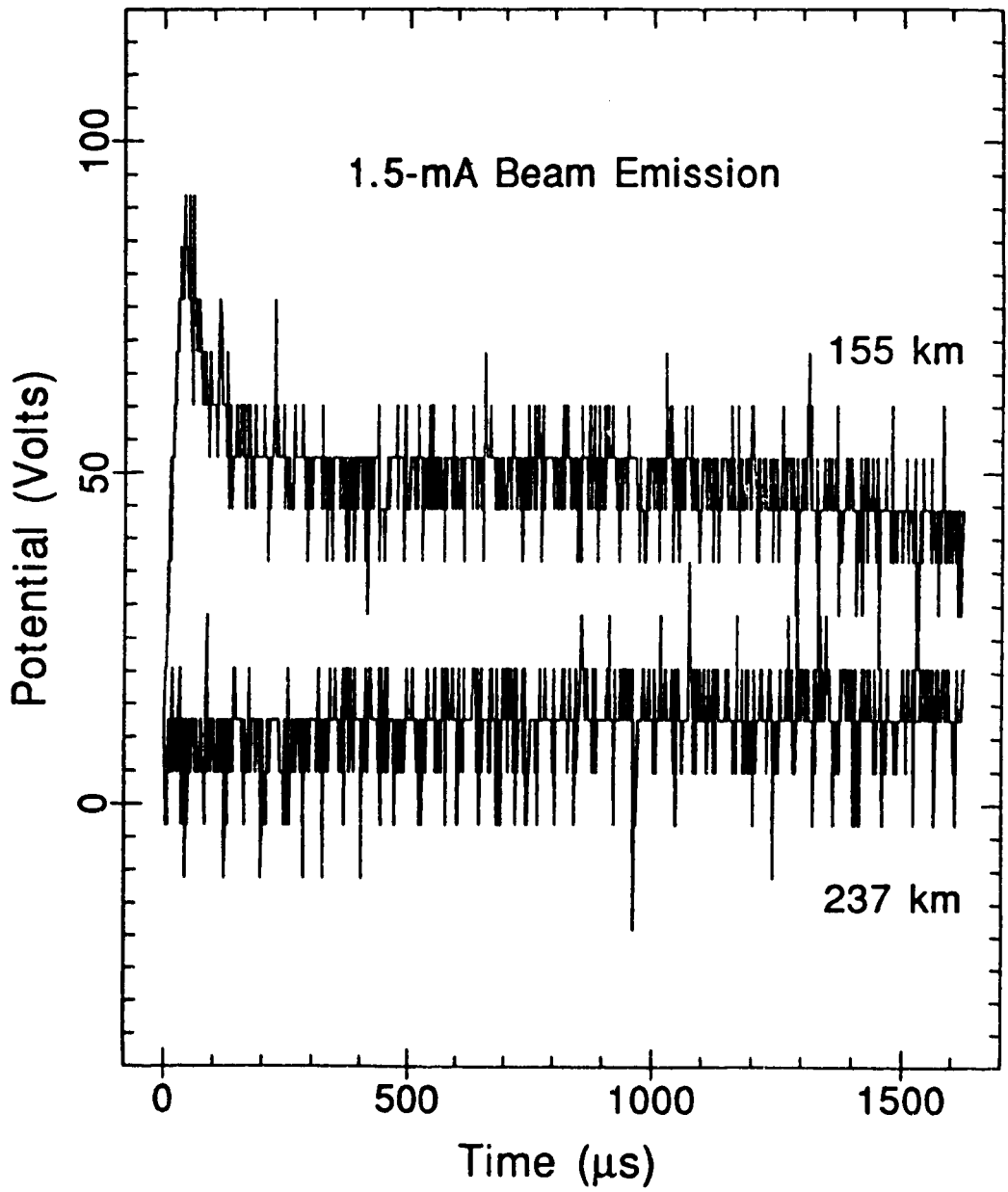


Figure 7

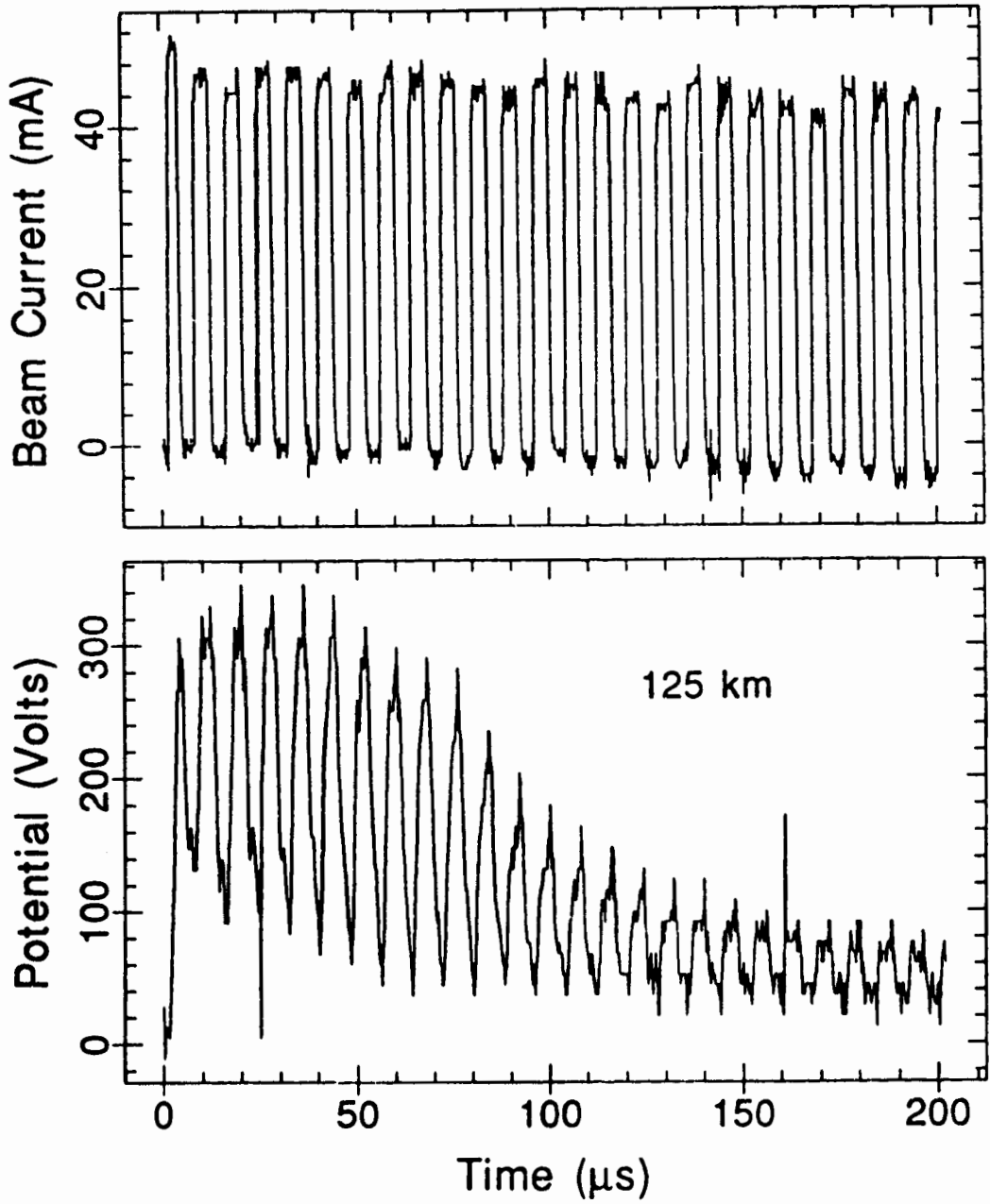


Figure 8